X-ray crystal structures of Al-doped (Y,Ca)Ba2Cu3O7-y whiskers

X-ray crystal structures of Al-doped (Y,Ca)$Ba_2Cu_3O_{7-y}$ whiskers

Federica Bertolotti,[a] Leandro Calore,[a] Giuliana Gervasio,[a*] Angelo Agostino,[a,b] Marco Truccato[b,c] and Lorenza Operti[a]

[a]Department of Chemistry and Centro Interdipartimentale di Cristallografia Diffrattometrica (CrisDi), University of Turin, Via P. Giuria 7, 10125 Turin, Italy,

[b]NIS Centre of Excellence, Via P. Giuria 7, 10125 Turin, Italy, and

[c]Department of Physics, University of Turin, Via P. Giuria 1, 10125 Turin, Italy

Correspondence e-mail: giuliana.gervasio@unito.it

Abstract

Al^{+3}-doped (Y,Ca)$Ba_2Cu_3O_{7-y}$ (YBCO) whiskers have been synthesized using a solid-state reaction technique. These materials are promising candidates for solid-state THz applications based on sequences of Josephson Junctions (IJJs). Alumina addition was systematically varied and the effect of aluminium incorporation on the structure has been investigated using single-crystal X-ray diffraction. Aluminium only replaces Cu atoms in the O-Cu-O-Cu chains and a gradual transition from orthorhombic to tetragonal space group occurs, thus increasing the Al content. A gradual modification of the coordination sphere of the copper site has also been observed. The Ca^{2+} ion substitutes mainly the Y^{3+} ion and also, to a small extent, the Ba^{2+} ion.

Keywords: whiskers; Al-doping; high-temperature superconductors; intrinsic Josephson junctions.

1. Introduction

In high-T_c superconductors (HTSC) such as $Bi_2Sr_2CaCu_2O_{8+\delta}$ (Bi-2212), $YBa_2Cu_3O_{7-\delta}$ (Y-123) and, more in general, RE-123 (RE = Y, Eu, Gd, Dy, Ho, Er, Tm and Lu), stacks of intrinsic Josephson junctions (IJJs) with atomic sizes are naturally present as a result of their crystal structure (Kleiner *et al.*, 1992; Kawae *et al.*, 2005; Okutsu *et al.*, 2008). A series of recent publications has shown that IJJs can be employed as the core components for the fabrication of several cryogenic micro-devices such as THz emitters (Ozyuzer *et al.*, 2007) and sensors (Wang *et al.*, 2001), micro-SQUIDs (Sandberg & Krasnov, 2005) and phase qubit applications based on the macroscopic quantum tunneling effect (Inomata *et al.*, 2005; Martinis *et al.*, 2005). Therefore, besides the needs related to the fundamental studies of structural and physical properties of HTSC, the growth of high-quality single crystals of these materials represents a crucial issue for their technological exploitation.

From this point of view, the possibility of growing crystals with high aspect ratios, also known as whiskers, has received considerable attention because of their highly crystalline nature, excellent superconducting properties and micrometric cross section area, which allow the fabrication of three-dimensional devices with a high degree of miniaturization (Okutsu *et al.*, 2008; Kawae, Kawae *et al.*, 2005; Pavlenko *et al.*, 2009; Inomata *et al.*, 2003).

While the growth of Bi-2212 whiskers in large amounts was reported soon after the discovery of HTSC (Matsubara *et al.*, 1989) and has been extensively studied (see for instance Badica *et al.*, 2006 for a review), Y-123 and RE-123 whiskers were successfully obtained only much later by Nagao *et al.* (2003, 2004) by making simultaneous use in the precursor powders of both Te and Ca as heteroelements. Although a different growth strategy was also explored by adding either Sb or Te as a single heteroelement (Nagao, Yun, Nakane *et al.*, 2005; Nagao *et al.*, 2010), the crystal yield remained very limited in all cases. On the contrary, a very recent experiment has shown that the addition of limited amounts of Al_2O_3 powder to the Te- and Ca-doped precursors remarkably increases the amount of grown Y-123 whiskers (Calore *et al.*, 2013). Of course, the presence of so many different elements raises questions about possible contaminations of the HTSC crystals during the growth process and the corresponding decrease of their superconducting properties, especially due to substitution of the Y and Ba elements by Te and Ca.

Actually, the influence of Ca doping in Y-123 has been widely studied from the point of view of its crystal structure both for polycrystalline material and for single crystals not grown with the whisker technique (Böttger *et al.*, 1997; Chen *et al.*, 2000; Stoyanova-Ivanova *et al.*, 2006; Hijar *et al.*, 1995). In principle, Ca should preferably substitute Y since the ionic radius of Ca^{2+} (r = 1.12 Å) is much closer to that of Y^{3+} (r = 1.019 Å) than to that of Ba^{2+} (r = 1.42 Å), and indeed X-ray structure refinements of single crystals have shown that at low Ca concentrations (< 11%) Y^{3+} ions are substituted, while at higher concentrations Ca^{2+} also replaces Ba^{2+} (Böttger *et al.*, 1997).

Concerning the Al addition, this element was either incorporated from alumina crucibles used during the synthesis of single crystals or added in the form of Al_2O_3 nanoparticles, showing a substantial effect on the structure and superconducting transition temperature in both cases (Antal *et al.*, 2010; Badica *et al.*, 2006; Oskina *et al.*, 1996). For instance, X-ray diffraction experiments on single crystals have shown that Al prefers an octahedral oxygen coordination, which is possible only in the Cu-O chains along the *b*-axis inducing a tetragonal *P*4/*mmm* crystal structure (Siegrist *et al.*, 1987). Other experiments applied neutron diffraction methods to investigate the effect of Al substitution in single crystals heated in different atmospheres on the oxygen excess and on the pinning effect induced by this cationic doping (Christensen *et al.*, 1992).

However, to the best of our knowledge, no study has been carried out about the combined effect on Y-123 of Al and Ca addition, or about their interaction with Te doping. This is the goal of the present paper, where we want to investigate the influence of such doping elements on the growth and the structural features of Y-123 whiskers by using a Y-123 Al-free one for comparison. It is also worth mentioning that whiskers should be considered as very good candidates for this kind of study because of their micro-crystalline nature and their well known low defectiveness, which are expected to give more precise indications about the structural effects of the different cationic substitutions. In spite of the fact that the superconducting properties of Y-123 whiskers have already been investigated to a good level of accuracy (Nagao *et al.*, 2006; De La Pierre *et al.*, 2009), quite unexpectedly their potential in terms of structural studies has been overlooked so far so that no X-ray structure refinement can be found in the literature for Y-123 whiskers. The present work also naturally fills this gap because of its design.

2. Experimental

2.1. Whiskers synthesis

Several methods were developed to grow single crystals of $YBa_2Cu_3O_{7-y}$; in this work a `self-flux method' has been used. Through this process high-quality crystals grow as a consequence of free nucleation (Schneemeyer *et al.*, 1987; Sun *et al.*, 1990; Ferretti *et al.*, 1994) from a high-temperature solid solution, where the flux is a mixture of oxides belonging to the Y-Ba-Cu-O phase diagram.

Powders were prepared by solid-state reaction of the individual components Y_2O_3 (99.999%), $BaCO_3$ (99.999%), CuO (99.9999%), $CaCO_3$ (99.9999%), TeO_2 (99.995%) and Al_2O_3 (99.998%) (Sigma-Aldrich, Germany) in the molar ratios Y:Ba:Cu:Ca:Te:Al = 1:2:3:1:0.5:(0.0-0.100). The precursor powders were thoroughly mixed and calcined at 1173 K in alumina crucibles for 10 h in air with three intermediate grindings. The calcined powders were then pressed into pellets of about 13 mm in diameter and 2 mm in thickness, which were subsequently put in a pure alumina boat and placed in a tube furnace for the thermal treatment. The nominal molar amounts of Al in the three precursor pellets used for different synthesis batches were 0 (batch 1), 0.025 (batch 2) and 0.100 (batch 3). A controlled oxygen flow (0.2 L min^{-1}) and a thermal cycle of T_{max} = 1278 K, t_{max} = 5 h and T_e = 1198 K for all the synthesis sets have been used, where T_{max} is the maximum temperature of the heating ramp, t_{max} is the dwell time at T_{max} and T_e is the end-point temperature of the cooling ramp, at which the oven has been turned off for furnace cooling. All the syntheses were performed following the constant heating and cooling rates of 5 K min^{-1} and 1 K per 60 min, respectively.

2.2. SEM/EDS analysis

Scanning electron microscope (SEM) and energy dispersive spectrometer (EDS) measurements were performed with a Zeiss EVO 10 equipped with the INCA Oxford software on the three whiskers selected from different batches [crystal (1) from the first batch; crystal (2) from the second batch and crystal (3) from the third batch], in order to obtain information about the morphologies and the cationic stoichiometries of the crystals. The acceleration voltage of the electron beam was 20 kV and the current used for the EDS analysis was 200 pA.

The corresponding stoichiometric composition determined *via* EDS measurements with the ZAF correction algorithm is shown in Table 1. Determination of possible Te content could not be performed due to the overlap of the corresponding peak with the Ca *K*α one. The oxygen content could not be evaluated accurately either.

Table 1
Stoichiometric composition for the three crystals corresponding to the different batches

The results have been normalized to (Y, Ca) = 1. The average error for each measurement is 0.01.

Nominal Al	Y	Ca	Ba	Cu	Al
0	0.88	0.12	1.77	2.78	0
0.025	0.87	0.13	1.92	2.72	0.08
0.100	0.88	0.12	1.78	2.57	0.31

It is worth noticing that the Al content measured for each crystal is greater than the nominal one by a factor of 3-4. On the contrary, the Ca intake is reduced by about a factor of 8 with respect to the starting composition, resulting in an actual content very similar to that reported in previous studies

(Nagao *et al.*, 2003, 2004; Calore *et al.*, 2013). Concerning the other elements, deviations from the ideal cationic ratios Y:Ba:(Cu,Al) = 1:2:3 are limited to less than about 0.23 for all the samples.

2.3. ICP-MS analysis

In order to discriminate between the presence or absence of Te in the crystals, inductively coupled plasma mass spectrometry (ICP-MS) analyses were performed with a Thermo Scientific (Waltham, MA) X5 Series spectrometer. The instrumental precision was better than 2% for trace elements, while the overall uncertainty, calculated on the basis of five genuine replicates, was better than 5%. Background signals were monitored at 5, 101 and 220 Da to perform a sensitivity test on the above-reported analyte masses. The limits of detection (LOD), calculated as three times the standard deviation of 11 blank measurements, and the limits of quantification (LOQ) result in the range of 0.6-2.9 ng L^{-1} by diluting multi-element solutions in 1% nitric acid solution. Internal standardization was used to correct for instrumental drifts by monitoring signals from ^{103}Rh, ^{115}In and ^{209}Bi isotopes, which were added to all samples, standards and blanks at a concentration level of 10 µg L^{-1}; responses from the three isotopes were interpolated to yield a better correction.

The resulting typical Te content was always less than 0.04 µg L^{-1}, corresponding to less than 0.03 in a stoichiometric ratio with the (Y, Ca) = 1 normalization. This outcome is in agreement with our EDS measurements and compatible with previous reports (Nagao *et al.*, 2003, 2004, 2010; Nagao, Yun, Wang *et al.*, 2005), clarifying that Te is not incorporated in the crystals during the whisker growth process. This fact has been used as input for the XRD refinement.

2.4. Single-crystal X-ray diffraction

Intensity data have been collected on a Gemini R Ultra diffractometer (Agilent Technologies UK Ltd) using an ω-scan technique ($\Delta\omega$ = 0.5°). *CrysAlis PRO* software (Agilent, 2012) has been used for data collection and reduction (peak intensities integration, background evaluation, cell parameters and space-group determination). Structure solution (direct methods) and refinement on F^2 have been performed by means of *SHELX*97 (Sheldrick, 2008). To understand the role of Al in the structure, an Al-free whisker (Babu *et al.*, 2006) has been measured for comparison [crystal (1)]. In Table 1 the experimental details and crystallographic data are reported for the three crystals.

2.4.1. Crystal (1)

The basic structure of Y-123 whiskers (space group *Pmmm*) is shown in Fig. 1. The structure has an yttrium ion in 1*h* Wickoff site (*mmm* symmetry) connected, according to a distorted cube, to eight oxygen ions, four O3 at a distance of 2.382 (6) Å and four O2 at 2.405 (5) Å. The Ba ion occupies the 2*t* Wickoff site (*mm*2) and it is surrounded by four O1 ions at 2.734 (1) Å, two O4 at 2.877 (1) Å, two O3 at 2.954 (7) Å and two O2 at 2.974 (7) Å. All the Ba-O distances are greater than the sum of Ba and O ionic radii (2.68 Å). Cu1 and Cu2 ions occupy the 1*a* (*mmm*) and the 2*q* (*mm*2) Wickoff sites, respectively. Cu1 achieves a planar environment with O1 and O4 ions, and Cu2 has a distorted planar coordination with O2 and O3 ions, and a weak interaction with O1 [2.307 (9) Å].

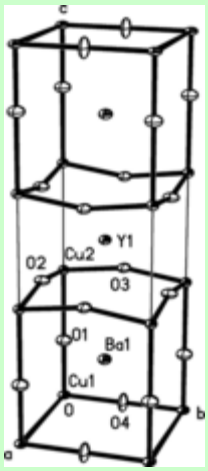

Figure 1
ORTEP plot of the unit cell of crystal (1), $(Y_{0.93},Ca_{0.07})Ba_2Cu_3O_{6.85}$ (displacement parameters at 50% probability).

If all ions with their occupancy factors (o.f.) are considered, the formula $YBa_2Cu_3O_7$ is obtained, which would not satisfy the charge neutrality of $YBa_2Cu_3O_{6.5}$ by assuming for Cu the usual +2 oxidation state. However, this is the situation that is normally found in Y-123, where the +3 oxidation state is theoretically possible for Cu and sometimes energetically favored in some lattice positions (Temmerman *et al.*, 2001), so that the compound is in general represented with the formula $YBa_2Cu_3O_{7-\delta}$.

Crystal (1) is Ca doped and Al free. The refinement was done allowing the Ca^{2+} to replace both Y^{3+} and Ba^{2+}. The refinement has shown that the Ca ion substitutes only Y ions as in other similar compounds (Nagao *et al.*, 2003; Hijar *et al.*, 1995); the obtained molar ratio Y/Ca is 0.93/0.07. At this stage a close inspection has been performed on the anisotropic displacement parameters; O2 and O4 ions have abnormally high displacement parameters with respect to the other O atoms and their o.f.s have been refined: only O4 has shown that the site occupancy is 0.85. The experimental formula of crystal (1) is therefore $(Y_{0.93},Ca_{0.07})Ba_2Cu_3O_{6.85}$. The presence of a residual peak (1.94 e $Å^{-3}$) at 0.50, 0.0, 0.0 is noteworthy because it corresponds to the so-called O5 peak introduced in some papers (Buttner *et al.*, 1992) and prefiguring the transition to the tetragonal symmetry where this position is occupied. The refinements introducing O5 give no significant result and also exclude partially twinned crystals.

Comparing these results with the stoichiometry $(Y_{0.88},Ca_{0.12})Ba_{1.77}Cu_{2.78}O_x$ resulting from EDS analysis it is apparent that they disagree well beyond the corresponding uncertainties. Deeper insight into this problem can be gained by considering that, in the conditions used for EDS analysis (*i.e.* 20 keV electrons at normal incidence with respect to the whisker *ab* surface), the CASINO Monte Carlo simulation of the electron trajectories shows that 95% of the signal comes from a layer within 1.2 µm from the crystal surface (Drouin *et al.*, 2007). On the other hand, in the same conditions of normal incidence, the attenuation length for the Mo $K\alpha$ radiation used for diffraction data acquisition is about 35.5 µm (Henke *et al.*, 1993). Comparing these lengths with the crystal thickness of 13 µm reported in Table 2, it is clear that the EDS analysis gives information only on the most external region of the crystal, while diffraction data reflect the average composition of the whole crystal. Analogue considerations also apply to the other crystals. In case of crystal (1) this means that the surface region of the whisker seems to be richer in Ca than the bulk one (Van Grieken & Markowicz, 2002).

Table 2
Crystal data and structure refinements for crystals (1), (2) and (3)

For all structures: Z = 1. Experiments were carried out at 293 K with Mo $K\alpha$ radiation using an Xcalibur, Ruby, Gemini ultra diffractometer. Refinement was with 0 restraints.

	Crystal (1)	**Crystal (2)**	**Crystal (3)**
Crystal data			
Chemical formula	$Ba_2Ca_{0.07}Cu_3O_{6.85}Y_{0.93}$	$Al_{0.06}Ba_2Ca_{0.06}Cu_{2.94}O_{6.81}Y_{0.94}$	$Al_{0.30}Ba_{1.92}Ca_{0.20}Cu_{2.70}O_{6.76}Y_{0.88}$
M_r	666.39	657.80	639.18
Crystal system, space group	Orthorhombic, *Pmmm*	Orthorhombic, *Pmmm*	Tetragonal, *P*4/*mmm*
a, *b*, *c* (Å)	3.8114 (3), 3.8712 (3), 11.6824 (7)	3.8380 (2), 3.8735 (2), 11.6947 (5)	3.8595 (2), 3.8595 (2), 11.6456 (8)
V (Å^3)	172.37 (2)	173.86 (2)	173.47 (2)
F(000)	291	290	282.7
D_x (g cm^{-3})	6.362	6.285	6.119
μ(mm^{-1})	28.11	27.77	26.38
Crystal size (mm)	0.18 × 0.07 × 0.01	0.21 × 0.04 × 0.02	0.24 × 0.04 × 0.02
Data collection			
Absorption correction	-	Analytical	Analytical
T_{min}, T_{max}	-	0.326, 0.639	0.304, 0.642
No. measured, independent and observed reflections	1081, 234, 220	1667, 353, 337	3659, 244, 228
R_{int}	0.044	0.026	0.040
$R\sigma$	0.034	0.017	0.014
$(\sin\theta/\lambda)_{max}$ (Å^{-1})	0.624	0.714	0.761
Refinement			
$R[F^2 > 2\sigma(F^2)]$, $wR(F^2)$, S	0.032, 0.083, 1.03	0.018, 0.051, 1.08	0.016, 0.039, 1.38
No. of reflections	234	353	233
No. of parameters	34	34	26
$\Delta\rho_{max}$, $\Delta\rho_{min}$ (e Å^{-3})	1.94, -1.32	0.90, -0.86	0.95, -1.19

Computer programs: *CrysAlis Pro* (Agilent, 2012), *SHELXS*97, *SHELXL*97 (Sheldrick, 2008).

2.4.2. Crystal (2)

The Ca substitution on Y and Ba ions gives results similar to that of crystal (1): the Ca ion only substitutes the Y ion in a molar ratio Y/Ca 0.94/0.06. This crystal also contains Al ions and the refinement shows that only Cu1 is substituted. The molar ratio Cu1/Al is 0.94/0.06. O4 shows high displacement parameters and its o.f. has been refined to a value of 0.66. A high residual peak (3.48 e Å^{-3}), corresponding to O5 has been introduced in the refinement with o.f. refined and U_{iso} fixed and *vice versa*. The refinement gives an o.f. of 0.15 for the O5 site. The refinements have shown that disorder between the positions of O4 and O5 is more reliable than twinning. So the formula of crystal (2) is $(Y_{0.94},Ca_{0.06})Ba_2(Cu_{2.94}, Al_{0.06})O_{6.81}$ (Fig. 2). Comparing this result with the EDS analysis, it seems that also in this case the surface region is richer in Ca than the interior of the crystal.

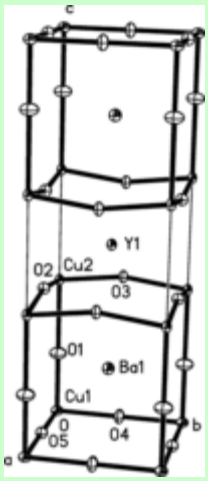

Figure 2
ORTEP plot of the unit cell of crystal (2), $(Y_{0.94},Ca_{0.06})Ba_2(Cu_{2.94},Al_{0.06})O_{6.81}$ (displacement parameters at 50% probability). Al^{+3} occupies the Cu1 position.

2.4.3. Crystal (3)

Crystal (3) (Fig. 3) has a quantity of Al greater than crystals (1) and (2). It belongs to the tetragonal space group *P*4/*mmm*. These facts correspond to different behavior for the Ca substitution compared with the previous crystals, because in this case Ca replaces both Y1 and Ba1 sites. On the other hand, no change occurs for the Al ions since the refinement shows that only Cu1 is substituted. For this crystal the refinement also shows abnormally high displacement parameters of O1 and O2 ions; in fact, the o.f.s of O1 and of O2 are reduced during refinement; the crystal structure of (3) is considered as pseudotetragonal in other papers (Sato *et al.*, 2001; Siegrist *et al.*, 1987). It is noteworthy that O2 positions correspond to those of O4 and O5 of the previous crystals (1) and (2). The formula obtained for crystal (3) is $(Y_{088},Ca_{0.12})(Ba_{1.92},Ca_{0.08})(Cu_{2.70}, Al_{0.30})O_{6.76}$.

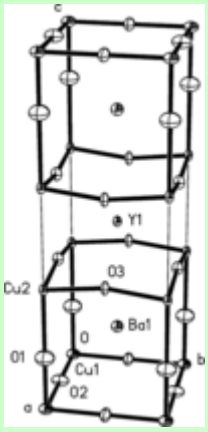

Figure 3
ORTEP plot of the unit cell of crystal (3), $(Y_{088},Ca_{0.12})(Ba_{1.92},Ca_{0.08})(Cu_{2.70},Al_{0.30})O_{6.76}$ (displacement parameters at 50% probability). Al^{+3} occupies the Cu1 position.

Comparison with EDS results of Table 1 is not straightforward for this crystal because of the different normalizations. However, converting both results into cationic percentages (*i.e.* excluding O that cannot be properly quantified by EDS), it turns out once more that the largest disagreement concerns Ca ions, confirming that the space distribution of this element is the most inhomogeneous in the crystal volume.

3. Results and discussion

Crystals (1), (2) and (3) are needle-shaped with the longest direction along the [010] axis. In Table 3 the interatomic distances for crystals (1), (2) and (3) are listed. Figs. 1 and 2 show the cell structures.

Table 3
Interatomic distances (Å) in crystals (1)-(3)

	Crystal (1)	Crystal (2)	Crystal (3)
Y1-O2	2.405 (5)	2.408 (2)	-
Y1-O3	2.382 (6)	2.395 (3)	2.405 (2)
Y1. . .Cu2	3.1994 (9)	3.2029 (4)	3.1956 (4)
Ba1-O1	2.734 (1)	2.7453 (5)	2.7526 (8)
Ba1-O2	2.974 (7)	2.964 (3)	2.9088 (3)
Ba1-O3	2.954 (7)	2.950 (3)	2.934 (2)
Ba1-O4	2.8775 (6)	2.8994 (3)	-
Ba1. . .Cu1	3.4680 (5)	3.4868 (2)	3.4907 (3)
Ba1. . .Cu2	3.380 (1)	3.377 (1)	3.374 (1)
Cu1-O1	1.843 (9)	1.852 (5)	1.817 (6)
Cu1-O2	-	-	1.9297
Cu1-O4	1.9356 (2)	1.9367	-
Cu1-O5	-	1.9190	-
Cu2-O1	2.307 (9)	2.314 (5)	2.343 (6)
Cu2-O2	1.924 (1)	1.9352 (5)	-
Cu2-O3	1.953 (1)	1.9525 (6)	1.9430 (4)

The cell parameters (Table 2) show a gradual increase of the *a* axis and a gradual approach of the *a*- and *b*-axis values, equal in the tetragonal cell, therefore confirming both the values and the general trend reported in recent studies (Calore *et al.*, 2013). The variation of cell parameters reflects the gradual appearance of the O5 ion inside the unit cell along the *a* axis (see Fig. 1). Crystal (1) is Ca^{2+}-doped; the small quantity of Ca^{2+}, however, does not affect the distances of (Y^{+3},Ca^{2+}) from the surrounding ions; the distances are equal to those of pure Y-123 (Sato *et al.*, 2001; Calestani & Rizzoli, 1987). The needle shape of the crystals along the [010] direction is justified by the presence along the *b* parameter of a double ...Cu1-O4-Cu1-O4... chain. In the *a* and *c* direction in fact there are also sequences of long Cu-Cu distances (Cu1-Cu1 3.811 and Cu2-Cu2 3.381 Å) and great separations among the layers due to the presence of yttrium and barium ions (see Fig. 1). Regarding the crystal morphology, it is noteworthy that in the tetragonal species there are two perpendicular sets of Cu-O chains, giving rise to a layer where the bonds are shorter. In fact in some cases it was found to be a platelet morphology of the tetragonal crystals (Siegrist *et al.*, 1987; Sato *et al.*, 2001; Nakai *et al.*, 1987).

Ca^{2+} doping is nearly constant in crystals (1) and (2) and Ca^{2+} occupies the Y^{3+} location. In crystal (3) the Ba^{2+} ion is also substituted [formula $(Y_{088},Ca_{0.12})(Ba_{1.92},Ca_{0.08})(Cu_{2.70},Al_{0.30})O_{6.76}$], in agreement with the statement that a greater quantity of Ca^{2+} also favors the Ba^{2+} substitution (Böttger *et al.*, 1997; Chen *et al.*, 2000).

The doping of $(Y,Ca)Ba_2Cu_3O_{7-y}$ with Al^{3+} shows the appearance of a peak at (0.5 0 0), already present and not significant in crystal (1) and with a relevant contribution in crystal (2). The

substitution of Al^{3+} in the Cu1 position [crystal (3)] therefore also gives rise to the formation of a roughly octahedral environment suitable for the allocation of Al^{3+} (see Fig. 3). Both Cu coordinations are greatly distorted owing to the well known Jahn-Teller effect. Crystal (2) can be considered to be intermediate between the orthorhombic and the tetragonal structure. Like a large number of whiskers that contain a relevant amount of Al or that are obtained warming the orthorhombic forms, crystal (3) has a tetragonal *P*4/*mmm* structure, as many RE-$Ba_2Cu_3O_{7-y}$ compounds are more or less doped (Siegrist *et al.*, 1987; Sato *et al.*, 2001; Nakai *et al.*, 1987; Jorgensen *et al.*, 1987; Sonntag *et al.*, 1991; Sasaki *et al.*, 1992); they have the *ab* basal plane oxygen-deficient. However, in crystal (3) the whole octahedron around (Cu, Al) is oxygen deficient. The main influence of Cu^{2+} substitution with Al^{3+} is shown by the Cu1-O1 and Cu2-O1 distances. In fact, owing to the greater charge of aluminium, O1 approaches Cu1 while Cu2-O1 increases (Table 3). The charge of Al^{3+} also affects the Ba1-Cu1 distance that in crystal (3) is significantly greater, while (Ba,Ca)-O1 is significantly shorter.

These results extend the previous observations on electrical resistivity by Calore *et al.* (2013), showing that the combined action of Al and Ca can modify the superconducting properties in a positive way compared with the action of Ca only, if the content of vicariant Al is about 0.06. On the other hand, the fact that higher contents (*i.e.* 0.30) of Al induce the semiconducting behavior of the crystals is also confirmed (see figure in the supporting information[1]).

4. Conclusions

Aluminium-doped (Y,Ca)-123 whiskers have been synthesized under the same conditions changing the alumina addition. The results of X-ray diffraction show the high quality of the whiskers and the good synthesis method. The effect of simultaneous Ca and Al co-doping on the Y-123 crystal structure has been clarified, showing that Ca replaces Y1 at any Al content, while Ba1 is substituted by Ca only at high Al additions and Al itself is incorporated in the structure only at the Cu1 site. A phase transition from an orthorhombic to a tetragonal space group and a gradual modification of the coordination sphere of the copper site occur with increasing Al content. In particular, a gradual increase of the percentage substitution of Cu1 sites has been found, when the alumina content in the precursor pellet increases. As a general conclusion for future applications, in order to maintain superconducting properties shown in the orthorhombic phase and suppressed in the tetragonal phase, a low value of Al (less than 11%) must replace the Cu1 site.

References

Agilent (2012). *CrysAlis PRO*, Version 1.171.35.19. Agilent Technologies, Yarnton, Oxfordshire, England.

Antal, V., Zmorayova, K., Kovac, J., Kavecansky, V., Diko, P., Eisterer, M. & Weber, H. W. (2010). *Supercond. Sci. Technol.* **23**, 065014. CrossRef

Babu, N. H., Iida, K., Shi, Y., Withnell, T. D. & Cardwell, D. A. (2006). *Supercond. Sci. Technol.* **19**, S461-S465. CrossRef

Badica, P., Togano, K., Awaji, S., Watanabe, K. & Kumakura, H. (2006). *Supercond. Sci. Technol.* **19**, R81-R99. CrossRef CAS

Böttger, G., Schwer, H., Kaldis, E. & Bente, K. (1997). *Physica C*, **275**, 198-204.

Buttner, R. H., Maslen, E. N. & Spadaccini, N. (1992). *Acta Cryst.* B**48**, 21-30. CrossRef details

Calestani, G. & Rizzoli, C. (1987). *Nature* **328**, 606-607. CrossRef CAS Web of Science

Calore, L., Rahman Khan, M. M., Cagliero, S., Agostino, A., Truccato, M. & Operti, L. (2013). *J. Alloys Compd.* **551**, 19-23. Web of Science CrossRef CAS

Chen, C., Wondre, F., Chowdhury, A. J. S., Hodby, J. W. & Ryan, J. F. (2000). *Physica C*, **341**,

589-592. CrossRef
Christensen, A. N., Hazell, R. G. & Grundvig, S. (1992). *Acta Chem. Scand.* **46**, 343-347. CrossRef
De La Pierre, M., Cagliero, S., Agostino, A., Gazzadi, G. C. & Truccato, M. (2009). *Supercond. Sci. Technol.* **22,** 045011. CrossRef
Drouin, D., Couture, A. R., Joly, D., Tastet, X., Aimez, V. & Gauvin, R. (2007). *Scanning*, **29**, 92-101. CrossRef PubMed CAS
Ferretti, M., Magnone, E. & Olcese, G. L. (1994). *Physica C*, **235**, 311-312. CrossRef
Henke, B. L., Gullikson, E. M. & Davis, J. C. (1993). *At. Data Nucl. Data Tables*, **54**, 181-342. CrossRef CAS
Hijar, C. A., Stern, C. L., Poeppelmeier, K. R., Rogacki, K., Chen, Z. & Dabrowski, B. (1995). *Physica C*, **252**, 13-21. CrossRef CAS
Inomata, K., Kawae, T., Nakajima, K., Kim, S. J. & Yamashita, T. (2003). *Appl. Phys. Lett.* **82**, 769-771. Web of Science® CrossRef CAS
Inomata, K., Sato, S., Nakajima, K., Tanaka, A., Takano, Y., Wang, H. B., Nagao, M., Hatano, H. & Kawabata, S. (2005). *Phys. Rev. Lett.* **95**, 107005-107009. Web of Science® CrossRef PubMed CAS
Jorgensen, J. D., Beno, M. A., Hinks, D. G., Soderholm, L., Volin, K. J., Hitterman, R. L., Grace, J. D., Schuller, I., Segre, C. U., Zhang, K. & Kleefisch, M. S. (1987). *Phys. Rev. B*, **36**, 3608-3616. CrossRef CAS
Kawae, T., Nagao, M., Takano, Y., Wang, H. B., Hatano, T. & Yamashita, T. (2005). *Physica C*, **426**, 1479-1483. CrossRef
Kleiner, R., Steinmeyer, F., Kunkel, G. & Muller, P. (1992). *Phys. Rev. Lett.* **68**, 2394-2397. CrossRef PubMed CAS Web of Science®
Martinis, J. M., Cooper, K. B., McDermott, R., Steffen, M., Ansmann, M., Osborn, K. D., Cicak, K., Oh, S., Pappas, D. P., Simmonds, R. W. & Yu, C. C. (2005). *Phys. Rev. Lett.* **95**, 210503-210506. Web of Science® CrossRef PubMed
Matsubara, I., Kageyama, H., Tanigawa, H., Ogura, T., Yamashita, H. & Kawai, T. (1989). *Jpn. J. Appl. Phys. Lett.* **28**, L1121-L1124. CrossRef CAS
Nagao, M., Kawae, T., Yun, K., Wang, H. B., Takano, Y., Hatano, T., Yamashita, T., Tachiki, M., Maeda, H. & Sato, M. (2005). *J. Appl. Phys.* **98**, 73903-73906. Web of Science® CrossRef
Nagao, M., Sato, M., Maeda, H., Yun, K. S., Takano, Y., Hatano, T. & Kim, S. (2003). *Appl. Phys. Lett.* **82**, 1899-1901. Web of Science® CrossRef CAS
Nagao, M., Sato, M., Tachiki, Y., Miyagawa, K., Tanaka, M., Maeda, H., Yun, K. S., Takano, Y. & Hatano, T. (2004). *Jpn. J. Appl. Phys.* **43**, L324-L327. Web of Science® CrossRef CAS
Nagao, M., Urayama, S., Kim, S. M., Wang, H. B., Yun, K. S., Takano, Y., Hatano, T., Iguchi, I., Yamashita, T., Tachiki, M., Maeda, H. & Sato, M. (2006). *Phys. Rev. B*, **74**, 054502-054506. CrossRef
Nagao, M., Watauchi, S., Tanaka, I., Okutsu, T., Takano, Y., Hatano, T. & Maeda, H. (2010). *Jpn. J. Appl. Phys.* **49**, 33101-33106. Web of Science® CrossRef
Nagao, M., Yun, K. S., Nakane, T., Wang, H. B., Takano, Y., Hatano, T., Yamashita, T., Tachiki, M., Maeda, H. & Sato, M. (2005). *Jpn. J. Appl. Phys.* **44**, L67-L70. Web of Science® CrossRef CAS
Nagao, M., Yun, K. S., Wang, H. B., Inomata, K., Kim, S., Takano, Y., Hatano, T., Yamashita, T., Tachiki, M., Maeda, H. & Sato, M. (2005). *IEEE Trans. Appl. Supercond.* **15**, 3169-3171. CrossRef CAS
Nakai, I., Sueno, S., Okamura, F. P. & Ono, A. (1987). *Jpn. J. Appl. Phys.* **26**, L788-L790. CrossRef CAS Web of Science®
Okutsu, T., Ueda, S., Ishii, S., Nagasawa, M. & Takano, Y. (2008). *Physica C*, **468**, 1929-1931. CrossRef CAS

Oskina, T. E., Ponomarev, Y. G., Piel, H., Tretyakov, Y. D. & Lehndorff, B. (1996). *Physica C*, **266,** 115-126. CrossRef CAS
Ozyuzer, L., Koshelev, A. E., Kurter, C., Gopalsami, N., Li, Q., Tachiki, M., Kadowaki, K., Yamamoto, T., Minami, H., Yamaguchi, H., Tachiki, T., Gray, K. E., Kwok, W. K. & Welp, U. (2007). *Science*, **318**, 1291-1293. Web of Science® CrossRef PubMed CAS
Pavlenko, V. N., Latyshev, Y. I., Chen, J., Gaifullin, M. B., Irzhak, A., Kim, S. J. & Wu, P. H. (2009). *JETP Lett.* **89**, 249-252. Web of Science® CrossRef CAS
Sandberg, M. & Krasnov, V. M. (2005). *Phys. Rev. B*, **72**, 212501-212504. CrossRef
Sasaki, S., Inoue, Z., Iyi, N. & Takekawa, S. (1992). *Acta Cryst.* B**48**, 393-400. CrossRef details
Sato, S., Kino, Y., Shibata, A., Nakamura, M., Krauns, C. & Shiohara, Y. (2001). *Acta Cryst.* C**57**, 341-343. CrossRef CAS details
Schneemeyer, L. F., Waszczak, J. V., Siegrist, T., Van Dover, R. B., Rupp, L. W., Batlogg, B., Cava, R. J. & Murphy, D. W. (1987). *Nature*, **328**, 601-603. CrossRef CAS Web of Science®
Sheldrick, G. M. (2008). *Acta Cryst.* A**64**, 112-122. CrossRef CAS details
Siegrist, T., Schneemeyer, L. F., Waszczak, J. V., Singh, N. P., Opila, R. P., Batlogg, B., Rupp, L. W. & Murphy, D. W. (1987). *Phys. Rev. B*, **36**, 8365-8368. CrossRef CAS
Sonntag, R., Hohlwein, D., Bruckel, T. & Collin, G. (1991). *Phys. Rev. Lett.* **66**, 1497-1500. CrossRef PubMed CAS Web of Science®
Stoyanova-Ivanova, A., Nedeltcheva, T., Dimitriev, Y., Kovachev, V., Terzieva, S., Vladimirova, B., Stanava, A. & Ignatov, H. (2006). *J. Univ. Chem. Tech. Met.* **41**, 25-28. CAS
Sun, B. N., Hartman, P., Woensdregt, C. F. & Schmid, H. (1990). *J. Cryst. Growth*, **100**, 605-614. CrossRef CAS Web of Science®
Temmerman, W. M., Winter, H., Szotek, Z. & Svane, A. (2001). *Phys. Rev. Lett.* **86**, 2435-2438. Web of Science® CrossRef PubMed CAS
Van Grieken, R. E. & Markowicz, A. A. (2002). *Handbook of X-ray Spectrometry*. New York: Dekker.
Wang, H. B., Wu, P. H. & Yamashita, T. (2001). *Phys. Rev. Lett.* **87**, 107002-107005. Web of Science® CrossRef PubMed CAS